



TITLE:

# Radiative lifetimes and coherence lengths of one-dimensional excitons in single-walled carbon nanotubes

AUTHOR(S):

Miyauchi, Yuhei; Hirori, Hideki; Matsuda, Kazunari; Kanemitsu, Yoshihiko

---

CITATION:

Miyauchi, Yuhei ...[et al]. Radiative lifetimes and coherence lengths of one-dimensional excitons in single-walled carbon nanotubes. Physical Review B 2009, 80(8): 081410(R).

ISSUE DATE:

2009-08

URL:

<http://hdl.handle.net/2433/87339>

RIGHT:

c 2009 The American Physical Society

# Radiative lifetimes and coherence lengths of one-dimensional excitons in single-walled carbon nanotubes

Yuhei Miyauchi,<sup>1,\*</sup> Hideki Hirori,<sup>2</sup> Kazunari Matsuda,<sup>1</sup> and Yoshihiko Kanemitsu<sup>1,3</sup>

<sup>1</sup>*Institute for Chemical Research, Kyoto University, Uji, Kyoto 611-0011, Japan*

<sup>2</sup>*Institute for Integrated Cell-Material Sciences, Kyoto University, Sakyo-ku, Kyoto 606-8501, Japan*

<sup>3</sup>*Photonics and Electronics Science and Engineering Center, Kyoto University, Kyoto 615-8510, Japan*

(Received 4 November 2008; revised manuscript received 27 July 2009; published 21 August 2009)

We evaluated the radiative lifetimes and the one-dimensional exciton coherence lengths in single-walled carbon nanotubes (SWNTs). The radiative lifetimes determined from simultaneous measurements of photoluminescence (PL) lifetimes and PL quantum yields range from  $\sim 3$  to 10 ns, and slightly increase with the tube diameter. The exciton coherence lengths in SWNTs are of the order of 10 nm, as deduced from the experimentally obtained radiative lifetimes, and they are about ten times larger than the exciton Bohr radius along the tube axis.

DOI: [10.1103/PhysRevB.80.081410](https://doi.org/10.1103/PhysRevB.80.081410)

PACS number(s): 78.67.Ch, 71.35.-y, 78.47.Cd, 78.47.jc

The optical properties of single-walled carbon nanotubes (SWNTs) are of great interest from a fundamental physics perspective, but also because of their potential applications as novel light-emitting materials for future optoelectronic devices. Because the excited electrons and holes are strongly confined in one-dimensional (1D) systems, the dynamics of the correlated electron-hole pairs (excitons) dominates the optical properties in semiconducting SWNTs.<sup>1,2</sup> The exciton spatial coherence volume (length) is defined as the volume from which the exciton can coherently capture the oscillator strength.<sup>3</sup> The exciton radiative lifetimes and the photoluminescence (PL) quantum yields are therefore dominated by the coherence volumes (lengths).<sup>3,4</sup> Moreover, the coherence lengths in SWNTs also determine whether the exciton motion can be treated as diffusive or not, which is the issue under intense debate.<sup>5-7</sup> This is directly related to the exciton relaxation mechanism and nonlinear optical properties<sup>8</sup> and therefore crucial for the future application of SWNTs as photonics devices such as light-emitting transistors and quantum light sources.<sup>9</sup>

The coherence length  $L_c$  is closely related to the radiative lifetime  $\tau_R$  and the homogeneous linewidth  $\Delta$ .<sup>3</sup>  $\tau_R$  can be estimated from the PL quantum yield  $\eta_{PL}$  and the PL decay time  $\tau_{PL}$ . For SWNTs, several experimental<sup>10-12</sup> and theoretical<sup>13,14</sup> studies of  $\tau_R$  have been reported. However, the measured values of  $\tau_R$  in each study show large scatter from  $\sim 10$  to 100 ns.<sup>10-12</sup> The sample-dependent large scatter in  $\eta_{PL}$  (0.01%–1%) for surfactant suspended SWNTs<sup>10-12,15</sup> has prevented us from determining  $\tau_R$  and  $L_c$  from the experimental results.

In this Rapid Communication we investigated the exciton radiative lifetimes of SWNTs using highly isolated SWNT ensembles with high PL quantum yields ( $\eta_{PL} \sim 1\%$ ), and determined the exciton coherence lengths from the radiative lifetimes. We measured the PL lifetimes and PL quantum yields of various  $(n, m)$  SWNTs simultaneously. The experimentally determined radiative lifetimes are typically 3–10 ns at room temperature. From the radiative lifetimes, we revealed that the exciton spatial coherence extends  $\sim 10$  nm along the tube axis.

The SWNTs were synthesized by the alcohol catalytic chemical vapor deposition method at 850 °C.<sup>16</sup> These

SWNTs were isolated by dispersion in a toluene solution with 0.07 wt% poly[9,9-dioctylfluorenyl-2,7-diyl] (PFO) (PFO-dispersed SWNTs), 60 min of moderate bath sonication, 15 min of vigorous sonication with a tip-type sonicator, and centrifugation at an acceleration of 13 000 g for 5 min, according to the procedure developed by Nish *et al.*<sup>17</sup> For comparison, we also prepared SWNTs by dispersion in D<sub>2</sub>O using 0.5 wt% sodium dodecyl benzene sulfonate (SDBS) (SDBS-dispersed SWNTs) with 30 min of vigorous sonication and ultracentrifugation at an acceleration of 150 000 g for 2 h, according to the procedure in Ref. 18.

We measured the PL lifetimes using the femtosecond excitation correlation (FEC) method. The FEC method has been successfully applied to a variety of materials, including SWNTs, to measure the recombination lifetimes of excitons.<sup>19-21</sup> In the FEC experiments, the SWNTs were excited with optical pulses from a Ti:sapphire laser of central wavelength 745 nm, repetition rate 80 MHz, pulse duration  $\sim 150$  fs, and spectral width 8 nm. The two beams separated by the delay time  $\tau$  were chopped at 800 and 670 Hz, respectively, and collinearly focused onto the same spot ( $\sim 10$   $\mu$ m). Only the PL signal components modulated at the sum frequency (1470 Hz) were detected as FEC signals with a photomultiplier and a lock-in amplifier after dispersion of PL by a monochromator. The measurements were carried out under the excitation condition  $\sim 100$   $\mu$ J/cm<sup>2</sup>. Detailed discussions on the PL lifetime measurement of SWNTs using FEC technique are presented in Ref. 20. The  $\eta_{PL}$  values of SWNTs were determined by comparison with those of the reference dyes (Styryl-13 and Rhodamine-6G).<sup>15</sup> The  $\eta_{PL}$  of Styryl-13 was calibrated against that of Rhodamine-6G in methanol ( $\eta_{PL} = 95\%$ ).

Figure 1(a) shows the absorption spectra of PFO-dispersed SWNTs and SDBS-dispersed SWNTs. The underlying background in the absorption spectrum of PFO-dispersed SWNTs is remarkably suppressed compared to that of the SDBS-dispersed SWNTs, and the absorption peaks are much more pronounced. This indicates that bundled SWNTs, residual impurities, or other amorphous and graphitic carbons were not included in the PFO-dispersed sample. Figure 1(b) shows the PL excitation (PLE) map of PFO-dispersed SWNTs. The absorption spectra and PLE spectra show that

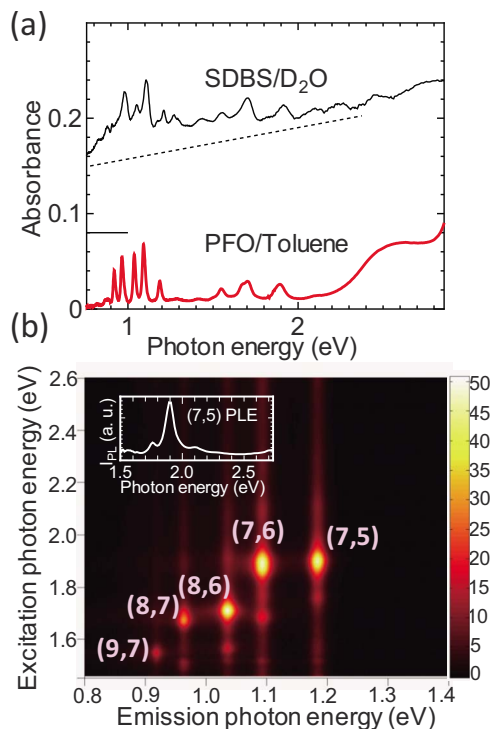


FIG. 1. (Color online) (a) Comparison of optical absorption spectra of SWNTs dispersed with SDBS in D<sub>2</sub>O and PFO in toluene. (b) PL excitation map of PFO-dispersed SWNTs. Inset shows the PLE spectrum of (7, 5) SWNTs.

only several types of chiral indices were included in the PFO-dispersed SWNTs samples. The diameters of SWNTs in the sample estimated from the absorption and PLE spectra range from  $\sim 0.8$  to  $1.2$  nm. The chiral indices of those peaks in the map are determined according to the assignment scheme described in Ref. 22.

In addition to the absorption spectrum with very low backgrounds, the small number of peaks enabled us to extract the  $\eta_{PL}$  of each  $(n,m)$  nanotube type in the PFO-dispersed sample. Figure 2(a) shows the absorption spectrum and the reconstructed spectrum based on the observed PLE spectrum. The reconstructed spectrum is the total of each  $(n,m)$  PLE spectrum, with only the amplitude of the peak varied as a fitting parameter. From the peak heights obtained in the fitting procedure, we determined the absorbance of each  $(n,m)$  peak at  $E_{22}$ . Figure 2(b) shows the evaluated  $\eta_{PL}$  of PFO-dispersed SWNTs as a function of tube diameter under the  $E_{22}$  resonance excitation conditions in each chiral index, where the relaxation rates from  $E_{22}$  to  $E_{11}$  were assumed to be independent of the chirality.<sup>23</sup> We estimated the  $\eta_{PL}$  to be from  $\sim 0.3\%$  to  $\sim 1.6\%$ , depending on the tube diameter. The relatively smaller diameter nanotubes have larger  $\eta_{PL}$  values, reaching  $\sim 1.6\%$  for (7, 5) SWNTs. This is consistent with a previous report on PFO-dispersed CoMoCAT SWNTs.<sup>17</sup>

Figure 3(a) shows the FEC signals as a function of delay time for (7, 5) SWNTs. The upward direction on the vertical axis indicates that the FEC signals have a negative sign. We checked that the FEC decay curves did not change by the excitation power density in the range from  $\sim 20$  to

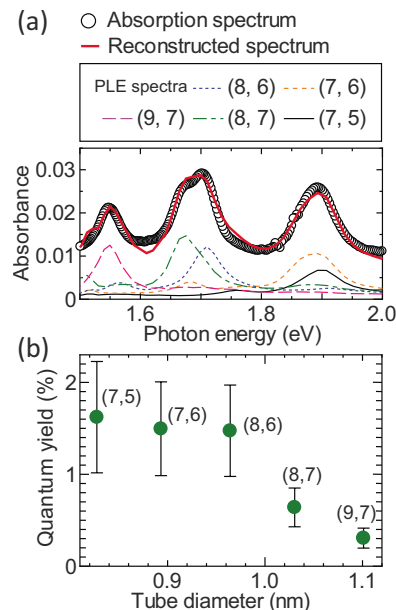


FIG. 2. (Color online) (a) Optical (circles) and decomposed (curves) absorption spectra of SWNTs with PFO in toluene using the PLE spectra of each  $(n,m)$  SWNT around the  $E_{22}$  transition. The red solid curve is the reconstructed absorption spectrum using PLE spectra of each  $(n,m)$ . (b) Measured PL quantum yields of PFO-dispersed SWNTs as a function of tube diameter.

$300 \mu\text{J}/\text{cm}^2$  [see inset of Fig. 3(a)]. The decay curve is closely described by a double exponential function (solid line) after subtracting the background signals. The exciton population showing double exponential decay as  $N_1(t) = C \exp(-t/\tau_A) + (1-C) \exp(-t/\tau_B)$  ( $0 \leq C \leq 1$  and  $\tau_A < \tau_B$ ) gives the FEC signal  $I_C(\tau)$  as

$$I_C(\tau) \propto -[C\tau_A \exp(-\tau/\tau_A) + (1-C)\tau_B \exp(-\tau/\tau_B)], \quad (1)$$

where  $C$  is the fractional amplitude of the fast decay component.<sup>20</sup> Here, we define the effective PL lifetime as  $\tau_{PL} = C\tau_A + (1-C)\tau_B$ , and the ratio of the fast component  $Y_A$  as  $Y_A = C\tau_A / [C\tau_A + (1-C)\tau_B]$ . For (7, 5) SWNTs in Fig. 3(a), we obtained  $Y_A \approx 0.7$ ,  $\tau_A \approx 45$  ps, and  $\tau_B \approx 200$  ps by the fitting procedure. These are similar to the recently reported values for single (6, 5) SWNTs in surfactant suspension.<sup>24</sup> The effective PL lifetime  $\tau_{PL}$  is calculated as  $\sim 60$  ps for (7, 5) SWNTs.<sup>21</sup> Figure 3(b) shows the effective PL lifetimes of PFO-dispersed SWNTs as a function of tube diameter. SWNTs with small diameters tended to have larger  $\tau_{PL}$ .

Figure 4 shows the experimentally derived radiative lifetimes  $\tau_R$  of SWNTs at room temperature as a function of tube diameter. The  $\tau_R$  are calculated from  $\eta_{PL}$  in Fig. 2(b) and  $\tau_{PL}$  in Fig. 3(b) as  $\tau_R = \tau_{PL} / \eta_{PL}$ . We found that the evaluated  $\tau_R$  are typically  $\sim 3$ – $10$  ns, and slightly increase with the tube diameter. From the obtained radiative lifetime at room temperature, the oscillator strength and the coherence length  $L_c$  of the 1D exciton states in SWNTs can be deduced. Note that the experimentally observed radiative decay rate  $\tau_R^{-1}$  does not simply correspond to that of the bright  $K_{ex}=0$  exciton  $\tau_0^{-1}$ , where  $K_{ex}$  is the exciton momentum. The oscillator strength of  $K_{ex}=0$  exciton is shared by all states within

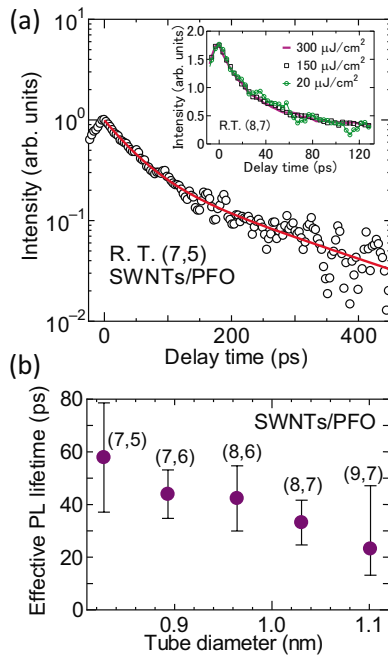


FIG. 3. (Color online) (a) The FEC signals for the (7, 5) SWNTs of the PFO-dispersed sample measured under 1.66 eV excitation at  $\sim 100 \mu\text{J}/\text{cm}^2$ . The red solid curve is given by a double exponential function. Inset shows the excitation power dependence of FEC curves for (8, 7) SWNTs from  $\sim 20$  to  $300 \mu\text{J}/\text{cm}^2$ . (b) The effective PL lifetimes  $\tau_{\text{PL}}$  as a function of tube diameter in the PFO-dispersed samples. Only the  $\tau_{\text{PL}}$  for the (9, 7) SWNTs was measured under 1.55 eV excitation to distinguish the PL signal of the (9, 7) SWNTs from that of the (8, 7) SWNTs.

the finite homogeneous linewidth  $\Delta(T)$  due to the uncertainty of  $K_{\text{ex}}$  induced by dephasing process,<sup>3</sup> and here we define the oscillator strength reduced by dephasing process as  $F_x$ . In addition, both the thermalization within each single exciton band, and the exciton distribution among bright and dark exciton states further reduce the  $F_x$  to the effective oscillator strength  $F_{x,\text{eff}}$ . We can obtain  $F_{x,\text{eff}}$  from the measured  $\tau_R$  as

$$F_{x,\text{eff}} = \frac{1}{\tau_R} \frac{2\pi\epsilon_0 m_0 \hbar^2 c^3}{n e^2 E_x^2}, \quad (2)$$

where  $n$  is the refractive index ( $\sim 1.5$  for toluene),  $m_0$  is the electron mass, and  $E_x$  is the exciton energy.

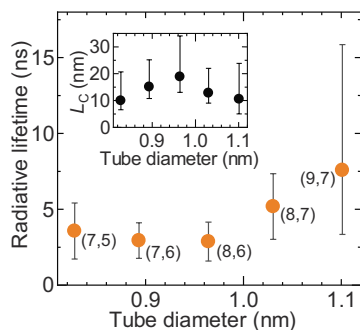


FIG. 4. (Color online) Determined radiative lifetimes  $\tau_R$  of SWNTs as a function of tube diameter. Inset shows deduced coherence lengths  $L_c$  as a function of tube diameter.

The fraction of excitons  $r_S(T)$  within  $\Delta(T)$  among the thermalized excitons in the bright exciton band can contribute to radiative recombination.  $r_S(T)$  is given by<sup>3</sup>

$$r_S(T) = \frac{\int_0^{\Delta(T)} D(E) e^{-E/k_B T} dE}{\int_0^{\infty} D(E) e^{-E/k_B T} dE}, \quad (3)$$

where  $D(E)$  is the exciton density of states. For the 1D case, assuming  $D(E) \propto 1/\sqrt{E}$ , we obtain  $r_S(T) = \text{erf}(\sqrt{\Delta/k_B T}) \sim \sqrt{\Delta/k_B T}$ . The  $T^{-1/2}$  dependence of the radiative decay rate has been observed in the temperature dependence in the PL measurements.<sup>25</sup> As mentioned above, the exciton distribution between singlet bright and dark states decreases  $F_x$  again by a factor of<sup>13,26</sup>

$$r_M(T) = e^{-\delta_1/k_B T} / (1 + e^{-\delta_1/k_B T} + 2e^{-\delta_2/k_B T}), \quad (4)$$

where  $\delta_1$  and  $\delta_2$  are the energy differences of the bright exciton and higher dark excitons measured from the bottom of the lowest singlet dark exciton band, respectively. Since the relationship between  $F_{x,\text{eff}}$  and  $F_x$  is expressed as  $F_x = r_S^{-1} r_M^{-1} F_{x,\text{eff}}$  using  $r_S(T)$  and  $r_M(T)$ , we thus determine the oscillator strength  $F_x$  from  $F_{x,\text{eff}}$ . Using experimentally obtained values of  $\Delta(T) \approx 13$  meV for a single nanotube at room temperature,<sup>27</sup>  $\delta_1 \approx 4$  meV,<sup>28</sup> and  $\delta_2 - \delta_1 \approx 30$  meV,<sup>29</sup> we obtain the factor  $r_S^{-1} r_M^{-1} \sim 6$  for (7, 5) SWNTs.

The  $F_x$  contains information on the exciton coherence length. The exciton coherence length  $L_c$  and the exciton oscillator strength  $F_x$  are related as  $L_c = F_x / f_0 |\phi(0)|^2$ , where  $f_0$  is the oscillator strength of a single  $k$ -state in the 1D momentum space, and  $\phi(z_e - z_h)$  denotes the envelope function of the electron-hole relative motion. In the 1D case,  $|\phi(0)|^2 \sim 1/a_x \sqrt{\pi}$ , where  $a_x$  is the exciton Bohr radius (exciton size). Using the theoretical derived value of  $a_x \approx 1.5$  nm (Ref. 30) and evaluating  $f_0 \approx 5$  according to Ref. 31, we evaluate the coherence length of excitons as  $L_c \sim 10$  nm in (7, 5) SWNTs.

Inset in Fig. 4 shows the evaluated coherence lengths for various  $(n, m)$  SWNTs. Here, we neglected the diameter dependence of  $\delta_2 - \delta_1$  because of their small contribution. We found that each  $(n, m)$  type has similar values of  $L_c \sim 10$  nm. These are in good agreement with the calculated values of  $L_c$  from the different formula using  $\Delta$  and the exciton effective mass.<sup>32</sup>

From our results, we can comment on the motion of excitons in SWNTs: The previously observed exciton excursion range of  $\sim 100$  nm (Ref. 7) is determined by the diffusive motion of the excitons because the  $L_c \sim 10$  nm is much smaller than the excursion range. The  $L_c$  also gives the saturation density  $N_S$  of excitons in SWNTs as  $1/N_S \sim L_c$ .<sup>32</sup> From  $L_c \sim 10$  nm, we get  $N_S \sim 10^2$  excitons/ $\mu\text{m}$  and this value is the upper limit of the exciton density in SWNTs at room temperature, which leads to the strong optical nonlinearity of SWNTs. Our experimental determination of  $L_c$  thus provides the further insight of the exciton transport and optical properties in SWNTs.

In conclusion, we have studied the exciton radiative lifetimes and coherence lengths in SWNTs. The radiative lifetimes of excitons at room temperature were experimentally



determined as 3 ~ 10 ns depending on the tube diameter. We found that the exciton coherence lengths were ~10 nm along the tube axis.

We thank S. Noda and K. Ishizaki, (Kyoto University); K. Sato (Tohoku University) and Shimadzu Corp. for measure-

ments and discussions. One of the authors (Y.M.) was financially supported by JSPS (Grant No. 20-3712). Part of this work was supported by JSPS KAKENHI (Grant No. 20340075) and MEXT KAKENHI (Grants No. 20048004 and No. 20104006).

\*Corresponding author; y.miyauchi@at7.ecs.kyoto-u.ac.jp

- <sup>1</sup>T. Ando, J. Phys. Soc. Jpn. **66**, 1066 (1997).
- <sup>2</sup>F. Wang, G. Dukovic, L. E. Brus, and T. F. Heinz, Science **308**, 838 (2005).
- <sup>3</sup>J. Feldmann, G. Peter, E. O. Gobel, P. Dawson, K. Moore, C. Foxon, and R. J. Elliott, Phys. Rev. Lett. **59**, 2337 (1987).
- <sup>4</sup>Y. Kanemitsu, K. Suzuki, Y. Nakayoshi, and Y. Masumoto, Phys. Rev. B **46**, 3916 (1992).
- <sup>5</sup>R. M. Russo, E. J. Mele, C. L. Kane, I. V. Rubtsov, M. J. The-rien, and D. E. Luzzi, Phys. Rev. B **74**, 041405(R) (2006).
- <sup>6</sup>L. Valkunas, Y. Z. Ma, and G. R. Fleming, Phys. Rev. B **73**, 115432 (2006).
- <sup>7</sup>L. Cognet, D. A. Tsyboulski, J.-D. R. Rocha, C. D. Doyle, J. M. Tour, and R. B. Weisman, Science **316**, 1465 (2007).
- <sup>8</sup>D. Song, F. Wang, G. Dukovic, M. Zheng, E. D. Semke, L. E. Brus, and T. F. Heinz, Appl. Phys. A: Mater. Sci. Process. **96**, 283 (2009).
- <sup>9</sup>A. Högele, C. Galland, M. Winger, and A. Imamoglu, Phys. Rev. Lett. **100**, 217401 (2008).
- <sup>10</sup>F. Wang, G. Dukovic, L. E. Brus, and T. F. Heinz, Phys. Rev. Lett. **92**, 177401 (2004).
- <sup>11</sup>M. Jones, C. Engtrakul, W. K. Metzger, R. J. Ellingson, A. J. Nozik, M. J. Heben, and G. Rumbles, Phys. Rev. B **71**, 115426 (2005).
- <sup>12</sup>A. Hagen, G. Moos, V. Talalaev, and T. Hertel, Appl. Phys. A: Mater. Sci. Process. **78**, 1137 (2004).
- <sup>13</sup>C. D. Spataru, S. Ismail-Beigi, R. B. Capaz, and S. G. Louie, Phys. Rev. Lett. **95**, 247402 (2005).
- <sup>14</sup>V. Perebeinos, J. Tersoff, and Ph. Avouris, Nano Lett. **5**, 2495 (2005).
- <sup>15</sup>J. Crochet, M. Clemens, and T. Hertel, J. Am. Chem. Soc. **129**, 8058 (2007).
- <sup>16</sup>Y. Miyauchi, S. Chiashi, Y. Murakami, Y. Hayashida, and S. Maruyama, Chem. Phys. Lett. **387**, 198 (2004).
- <sup>17</sup>A. Nish, J.-Y. Hwang, J. Doig, and R. J. Nicholas, Nat. Nano-technol. **2**, 640 (2007).
- <sup>18</sup>M. J. O'Connell *et al.*, Science **297**, 593 (2002).
- <sup>19</sup>H. Hirori, K. Matsuda, Y. Miyauchi, S. Maruyama, and Y. Kanemitsu, Phys. Rev. Lett. **97**, 257401 (2006).
- <sup>20</sup>Y. Miyauchi, K. Matsuda, and Y. Kanemitsu, arXiv:0906.3381 (unpublished), and references therein.
- <sup>21</sup>We have confirmed that the effective PL lifetime of (7, 5) SWNTs measured by the FEC method (~60 ps) is agree well with the value (~64 ps) measured by PL decay measurement using a streak camera.
- <sup>22</sup>S. M. Bachilo, M. S. Strano, C. Kittrell, R. H. Hauge, R. E. Smalley, and R. B. Weisman, Science **298**, 2361 (2002).
- <sup>23</sup>S. Lebedkin, F. Hennrich, O. Kiowski, and M. M. Kappes, Phys. Rev. B **77**, 165429 (2008).
- <sup>24</sup>S. Berciaud, L. Cognet, and B. Lounis, Phys. Rev. Lett. **101**, 077402 (2008).
- <sup>25</sup>I. B. Mortimer and R. J. Nicholas, Phys. Rev. Lett. **98**, 027404 (2007).
- <sup>26</sup>The exciton distribution between bright and dark states might not be necessarily thermalized due to finite scattering rate between bright and dark states. However, this contribution is small at room temperature, and therefore we assume the Boltzmann distribution of excitons here.
- <sup>27</sup>K. Yoshikawa, R. Matsunaga, K. Matsuda, and Y. Kanemitsu, Appl. Phys. Lett. **94**, 093109 (2009).
- <sup>28</sup>R. Matsunaga, K. Matsuda, and Y. Kanemitsu, Phys. Rev. Lett. **101**, 147404 (2008).
- <sup>29</sup>Y. Miyauchi and S. Maruyama, Phys. Rev. B **74**, 035415 (2006).
- <sup>30</sup>R. B. Capaz, C. D. Spataru, S. Ismail-Beigi, and S. G. Louie, Phys. Rev. B **74**, 121401(R) (2006).
- <sup>31</sup>A. Grüneis, R. Saito, G. G. Samsonidze, T. Kimura, M. A. Pimenta, A. Jorio, A. G. Souza Filho, G. Dresselhaus, and M. S. Dresselhaus, Phys. Rev. B **67**, 165402 (2003); A. Grüneis, Ph.D. Thesis, Tohoku University, 2004.
- <sup>32</sup>T. Takagahara, Solid State Commun. **78**, 279 (1991).